Effect of Molecular Weight Distribution on the Shear Dependence of Viscosity in Polymer Systems

WILLIAM W. GRAESSLEY and LEON SEGAL

Northwestern University, Evanston, Illinois

The viscosity of concentrated solutions of polystyrene were measured in steady shearing flow with a Weissenberg rheogoniometer. The polymers ranged in weight average molecular weight $\overline{M}_w$ from 97,000 to 3,370,000 and in distribution breadth $\overline{M}_w/\overline{M}_n$ from 1.05 to 3.1. The solvent was *n*-butylbenzene, and the solutions ranged in concentration from 0.20 to 0.55 g./cc. These data were supplemented by measurements on bulk polystyrenes and polyethylenes with distribution breadths as high as $\overline{M}_w/\overline{M}_n = 20$. Master curves of reduced viscosity vs. reduced shear rate were calculated theoretically for each molecular weight distribution. The experimental viscosity data superimposed satisfactorily on these curves and furnished the viscosity at zero shear rate η_0 and an experimental time constant τ_0 for each solution. The time constant paralleled closely the Rouse relaxation time τ_R in all systems. Residual variations in the ratio τ_0/τ_R with molecular weight and concentration correlated uniquely with the product $c\overline{M}_w$. These results indicate that the viscosity behavior of a polymer can be predicted with reasonable accuracy from data on its molecular weight distribution.

Many studies have been made in recent years on the non-Newtonian behavior of polymers in steady shearing flow. In most cases, commercially available materials were used, and very little information on molecular structure was measured or reported. The development and refinement of analytical methods such as light scattering, osmometry, and gel permeation chromatography has made molecular information more generally available than before, and it has become increasingly evident that such structural features as average molecular weight, molecular weight distribution, and degree of chain branching have important influences on the macroscopic behavior of polymer systems. The purpose of this paper is to examine experimental viscosity data on several well-characterized polymer samples and to relate the behavior to the known structure of the samples.

The viscosity of amorphous polymers and concentrated polymer solutions depends on shear rate, and this dependence is rather similar for a wide range of systems. At sufficiently low shear rates, the viscosity η is independent of the shear rate $\dot{\gamma}$. At somewhat higher shear rates, the viscosity decreases with increasing shear rate, many times approaching power-law behavior $\eta = (\text{const.}) \mid \dot{\gamma} \mid^{-a}$ over a moderate range of shear rates. At still higher shear rates, a lower limiting viscosity appears, but in concentrated systems this region is seldom observable.

The magnitude of the zero shear viscosity η_0 depends on temperature, polymer concentration, chain length, and chain length distribution. The relationships are reasonably well understood for linear polymers, at least in broad outline (*7, 8*). However, the effect of molecular variables on the entire viscosity vs. shear rate curve is less certain. Considerable controversy still surrounds even the question of what molecular mechanisms are responsible for the non-Newtonian properties of polymer systems. Nevertheless, the behavior is reasonably systematic, particularly if attention is restricted to concentrated systems of linear, high molecular weight polymers.

If measurements are made with the same polymer sample at different temperatures or at different concentrations in an inert diluent, the experimental viscosity curves can usually be made to superimpose and conform to a single master curve. Suitable normalizing factors for constructing the master curve are the zero shear viscosity η_0 and a characteristic shear rate $\dot{\gamma}_0$, locating in a consistent way the range of shear rates where the viscosity coefficient begins to deviate from its zero shear value. The form of the master curve depends on the distribution of molecular weights in the polymer (*16, 20, 22, 23*). Thus

$$\eta/\eta_0 = V(\dot{\gamma}/\dot{\gamma}_0) \tag{1}$$

and the function V depends only on the form of the distribution function $P(n)$, the fractional number of polymer chains in the system with n repeating units.

The reciprocal of $\dot{\gamma}_0$ has the units of time and is generally found to be of the order of the Rouse or Bueche molecular relaxation times for the system (*3, 4*)

$$\frac{1}{\dot{\gamma}_0} = \tau_0 = K\tau_R \tag{2}$$

and for polymers of narrow molecular weight distribution

$$\tau_R = \frac{6}{\pi^2}\,\frac{\eta_0 M}{cRT} \tag{3}$$

The Bueche relaxation time τ_B is simply $2\tau_R$. Recent experiments on solutions of narrow distribution polystyrene (*12*) have shown that K is not a constant but varies from sample to sample such that

$$\tau_0 = \frac{\alpha\tau_R}{1 + \beta\ cM} \tag{4}$$

in which α and β are constants.

Commercial polymers typically have broad molecular distributions, and they are almost invariably processed in the amorphous state, either in bulk or as concentrated solutions. Methods are available for measuring average molecular weight and molecular weight distribution, and it would be highly desirable to be able to predict the form of the viscosity master curve for such information. The experimental studies reported here will be examined in

Leon Segal is at Brooklyn Polytechnic Institute, Brooklyn, New York.

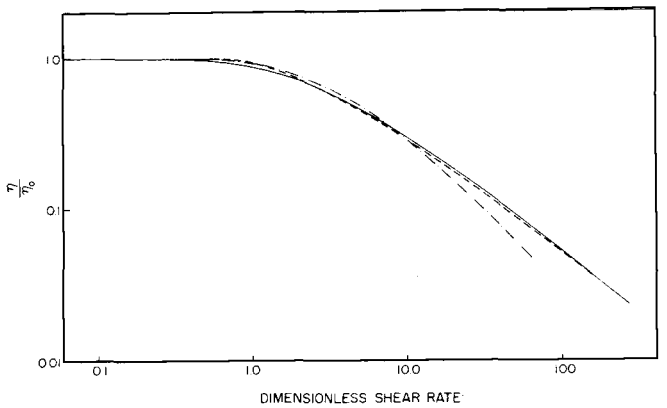

Fig. 1. Viscosity master curves for monodisperse systems. The solid line (——) is from Ree-Eyring (22); the dashed line (- - -) is from Graessley (11); the construction line (—·—·—) is from Williams (25).

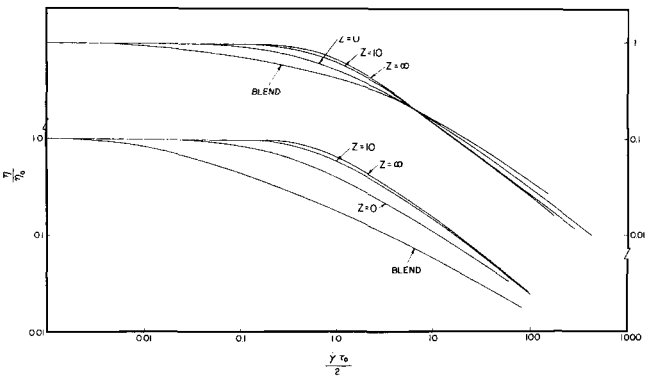

Fig. 2. Viscosity master curves for polydisperse systems. The upper set of curves was calculated with Middleman's equation [Equation (9)], and the viscosity scale for these curves is on the right. The lower set was calculated from the entanglement theory; the viscosity scale for these is on the left.

the light of recent theories of viscosity in polydisperse systems. Both the superposability of experimental and theoretical master curves and the subsequent correlation of the experimental time constants from samples with different distributions will be considered.

THEORIES OF NON-NEWTONIAN BEHAVIOR

Molecular chain entanglement refers to the physical interaction between polymer molecules during flow and the resistance to relative motion beyond that of ordinary segmental drag, arising from the connectedness of the repeating units in the individual molecules (20). The need to consider chain entanglements grew first out of attempts to explain deviations from the kinetic theory of rubber elasticity, according to which the number of elastically active chain segments was found to be greater than the chemical cross-linking density (6). Entanglements were subsequently invoked for noncross-linked systems to explain both the sharp increase in the molecular weight dependence of melt viscosity beyond a critical value M_c and the concomitant appearance of a rubberlike plateau in the creep and stress relaxation moduli (2, 5). The invariance of M_c with temperature in many systems indicated a physical rather than a chemical interaction, and the constancy of the product cM_c in concentrated solutions suggested an interaction that increases in direct proportion to the chain lengths of the individual molecules. The postulation of a deformable transient network of entangled but chemically distinct molecules also has provided a qualitative explanation for the memory and elastic behavior of flowing polymer systems (18).

In steady shearing flow, the environment of any polymer molecule in the fluid is constantly being renewed in the sense that the flow sweeps other molecules continually into and out of its sphere of influence. The drag forces associated with this relative motion control the magnitude of the viscosity coefficient. In highly entangled systems, the drag forces derive mainly from physical couples which exist temporarily between passing chains. If a finite time is required to develop effective couples between passing chains, then the net number of couples per molecule will depend on the shear rate. According to this view, the decrease in viscosity with shear rate is simply a consequence of the net decrease in entanglement density induced by flow.

A quantitative theory of non-Newtonian behavior based on an elaboration of this idea has been presented (10, 11). With the equations from this theory, a viscosity-shear rate master curve can be calculated for any specified distribution of molecular weights. Thus

$$\frac{\eta}{\eta_0} = \frac{\int_0^\infty n^2 h(\dot\gamma, n)\, P(n)dn \int_0^\infty n^{7/2}\, g^{5/2}(\dot\gamma, n)\, P(n)dn \int_0^\infty nP(n)dn}{\int_0^\infty n^2\, P(n)dn \int_0^\infty ng(\dot\gamma, n)\, P(n)dn \int_0^\infty n^{7/2}\, P(n)dn} \tag{5}$$

where

$$g(\dot\gamma, n) = \frac{2}{\pi}\left[\cot^{-1}\theta + \frac{\theta}{1+\theta^2}\right] \tag{6}$$

and

$$h(\dot\gamma, n) = \frac{2}{\pi}\left[\cot^{-1}\theta + \frac{\theta(1-\theta)^2}{(1+\theta^2)^2}\right] \tag{7}$$

The variable $\theta(\dot\gamma, n)$ is defined implicitly for each choice of n and $\dot\gamma$ by the equation

$$\theta = \left(\frac{\dot\gamma\tau_0}{2}\right)\left(\frac{\eta}{\eta_0}\right)\left(\frac{n}{n_w}\right)^2 h(\theta)\,\frac{\int_0^\infty n^2\, P(n)dn}{\int_0^\infty n^2\, h(\dot\gamma, n)\, P(n)dn} \tag{8}$$

The parameter τ_0 is a characteristic relaxation time, related to the time to form entanglement couples in the undisturbed system, and defined as in Equations (2) and (3) with M replaced by the weight average molecular weight $\overline{M}_w$. In Equation (8), n_w is the weight average number of repeating units per chain.

Middleman has suggested another method for calculating master curves which is not based on any specific molecular model. In this approach, the behavior of monodisperse systems must be furnished, either experimentally or by some other theory. Once available, the monodisperse master curve is summed over all molecules in the system and normalized, the weighting of the various components being made according to the original Rouse and Bueche models. In the terminology of the present article, the Middleman equation becomes

TABLE 1. POLYMER SAMPLES USED IN THE STUDY*

$\overline{M}_w$	$(\overline{M}_w/\overline{M}_n)$	$\frac{\overline{M}_z\overline{M}_{z+1}}{\overline{M}_w^2}$†	Source of Data or Sample
48,500	1.08	1.25	Stratton data
97,000	1.06	1.25	Pressure Chemical Company
117,000	1.07	1.25	Stratton data
160,000	1.06	1.25	Pressure Chemical Company
160,000	9.7	49	Polyethylene, Chemplex Company data
179,000	1.07	1.25	Stratton data
192,000	12.2	89	Polyethylene, Chemplex Company data
198,000	16.6	71	Polyethylene, Chemplex Company data
209,000	2	3	Thermal polymerization at 120°C. in ethyl benzene
217,000	1.09	1.25	Stratton data
241,000	2	3	Thermal polymerization at 120°C. in ethyl benzene
242,000	1.03	1.25	Stratton data
371,000	2.74	7.6	Shell Development Company data
411,000	1.01	1.25	Pressure Chemical Company
418,000	3.1	22.5	Blend of thermal polymers: 87% by weight of $\overline{M}_w = 241{,}000$ and 13% of $\overline{M}_w = 1{,}600{,}000$.
677,000	2	3	Thermal polymerization at 100°C. in bulk
860,000	1.20	1.25	Pressure Chemical Company
1,600,000	2	3	Thermal polymerization at 60°C. in bulk
1,900,000	2	3	Thermal polymerization at 60°C. in bulk
2,400,000	1.1	1.25	Fractionation of 60°C. thermal polymer
3,370,000	2	3	Thermal polymerization at 40°C. in bulk

* Polystyrene unless otherwise indicated.
† Estimated from the assumed form of the distribution or calculated from the gel permeation chromatograph data. In either case, the values must be regarded as nominal and only approximate.

$$\frac{\eta}{\eta_0} = \frac{\int_0^\infty n^2 P(n)\, \varphi\left(\frac{\dot\gamma\tau_0}{2}\left(\frac{n}{n_w}\right)^2\right) dn}{\int_0^\infty n^2 P(n) dn} \tag{9}$$

The function $\varphi\left(\frac{\dot\gamma\tau_0}{2}\right)$ is the master curve for a monodisperse system, and $\tau_0/2$ is the time constant of the system. The parameter $\frac{\tau_0}{2}\left(\frac{n}{n_w}\right)^2$ in the argument of φ in Equation (9) comes from the relative relaxation time of a chain of size n in a polydisperse system of Rouse chains of weight average size n_w:

$$\tau_R(n) = \frac{6}{\pi^2}\left(\frac{\eta_0 M^2}{cRT\,\overline{M}_w}\right) \tag{10}$$

$$= \frac{6}{\pi^2}\frac{\eta_0\,\overline{M}_n}{cRT}\left(\frac{\overline{M}_n}{\overline{M}_w}\right)\left(\frac{n}{n_n}\right)^2 \tag{11}$$

$$= \frac{6}{\pi^2}\frac{\eta_0\,\overline{M}_w}{cRT}\left(\frac{n}{n_w}\right)^2 \tag{12}$$

Where Middleman used τ_B explicitly, we have substituted $\tau_0/2$. He also chose to form his relaxation time with $\overline{M}_n$ [Equation (11)]. To make both theories as directly comparable as possible, we have cast his representation of the time constant of the system τ_0 in the completely equivalent form involving $\overline{M}_w$ [Equation (12)].

If the distribution function $P(n)$ is given either by an analytical expression or in the form of experimental data, the normalized viscosity shear rate curve can be obtained. For the entanglement theory, Equation (8) can be written as

$$\theta = F(\dot\gamma)\left(\frac{n}{n_w}\right)^2 h(\theta) \tag{13}$$

where

$$F(\dot\gamma) = \left(\frac{\eta}{\eta_0}\right)\left(\frac{\dot\gamma\tau_0}{2}\right)\frac{\int_0^\infty n^2 P(n) dn}{\int_0^\infty n^2 h(\dot\gamma, n)\, P(n) dn} \tag{14}$$

A value of $F(\dot\gamma)$ is chosen first, and values of θ are calculated for individual values of (n/n_w) by some suitable numerical procedure. The functions $h(\theta)$ and $g(\theta)$ are then evaluated for each (n/n_w), and the integrals in Equation (5) are calculated numerically. The resulting values of η/η_0 and $\int_0^\infty n^2 P(n) dn / \int_0^\infty n^2 h(\dot\gamma, n)\, P(n) dn$ are finally used to calculate the reduced shear rate $\dot\gamma\tau_0/2$ from the originally chosen value of $F(\dot\gamma)$. This procedure is repeated for other values of $F(\dot\gamma)$, thereby generating a complete curve of η/η_0 vs. $\dot\gamma\tau_0/2$ for the distribution function $P(n)$ originally chosen.

Middleman's equation can be integrated quite simply once a suitable master curve expression for monodisperse systems is selected. Figure 1 shows the behavior according to three different theories: the entanglement theory (*11*), the Ree-Eyring theory for a single relaxing flow element (*22*), and the intermolecular interaction theory of Williams (*25*). The three results are quite similar, and all fit the data on narrow distribution polymers rather well. We selected the monodisperse curve of the entanglement theory to make the calculations with Equation (9). In this way both polydisperse theories begin from the same point, and their relative ability to average correctly as the distribution broadens can be fairly gauged.

Master curves for the Schulz-Zimm model distribution

$$P(n) = \frac{(Z+2)^{Z+1}}{n_w\,(Z!)}\left(\frac{n}{n_w}\right)^Z \exp\left[-\left(\frac{n}{n_w}\right)(Z+2)\right] \tag{15}$$

were calculated by both theories and are shown in Figure

2 for various values of the distribution parameter Z. The value Z = 0 corresponds to the commonly observed case of a most probable distribution of molecular weights ($\overline{M}_w/\overline{M}_n = 2$), while Z = ∞ corresponds to a monodisperse system ($\overline{M}_w/\overline{M}_n = 1$). Also shown is a curve calculated for a blend of two samples with most probable distribution (see experimental methods). This sample has $\overline{M}_w/\overline{M}_n = 3.1$ and a large high molecular weight tail.

Both theories show that broadening the distribution causes deviations from the zero shear viscosity at lower shear rates and results in a smaller slope over a large portion of the high shear region. Furthermore, calculations with other model distributions have shown that the higher molecular weight averages such as $\overline{M}_w$ and $\overline{M}_z$ are much more important than $\overline{M}_n$ in controlling the shape of the master curve. These results are consistent with experimental observations (*17, 21*), particularly with the recent suggestion that the property of the distribution most relevant to viscosity behavior is $\overline{M}_z\overline{M}_{z+1}/\overline{M}_w^2$ (*14*).

The difference between the sets of curves are of two kinds: the relative positions of individual curves and their shapes. Curves from the entanglement theory shift rapidly to lower shear rates as the distribution broadens and approach the monodisperse curve again only at very high shear rates. Curves from the Middleman equation are not shifted as far by polydispersity and actually cross the monodisperse curve at intermediate η/η_0 values. If this were the only variation, that is, if the shapes of the curves for samples of a given distribution were the same according to the two theories but only shifted differently relative to the monodisperse curve, then the theories would be equivalent, except for the numerical values of the time constant τ_0 obtained. However, there are also systematic differences in shape as the distribution broadens. The monodisperse curves ($\overline{M}_z\overline{M}_{z+1}/\overline{M}_w^2 = 1.0$) are, of course, identical; the curves for most probable distribution ($\overline{M}_z\overline{M}_{z+1}/\overline{M}_w^2 = 3.0$) are practically the same, but the curves for the blend ($\overline{M}_z\overline{M}_{z+1}/\overline{M}_w^2 = 22.5$) are significantly different. The Middleman curve is flatter at η/η_0 values near unity, that is, it possesses a longer tail at low shear rates, and it decreases more steeply at high shear rates. As will be seen, these differences persist in the calculated master curves for other samples with broad distribution.

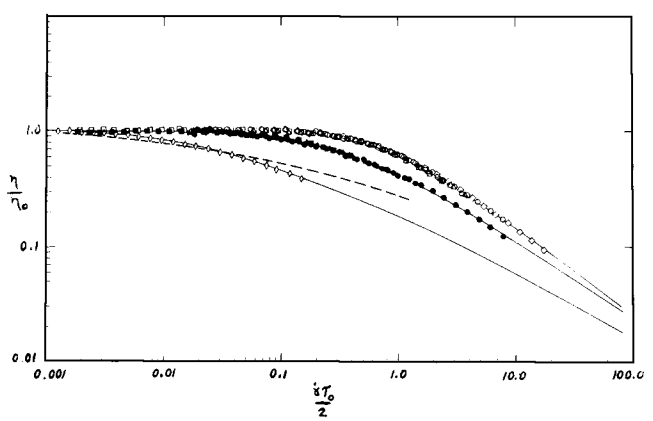

Fig. 3. Viscosity data on polystyrene solutions. The curve on the right (open circles, squares, triangles, hexagons) is the datum for narrow distribution samples superimposed on the master curve for Z = 10. The middle curve (closed circles, hexagons, etc.) is the datum for broad distribution samples superimposed on the master curve for Z = 0. The curve on the left (open diamonds) is the datum on the blend superimposed on the blend master curve from the entanglement theory. The dashed line is the master curve from equation (9), shifted to fit the data as well as possible.

EXPERIMENTAL METHODS

Narrow distribution samples of polystyrene were prepared by an anionic polymerization procedure. The sample of highest molecular weight was obtained by precipitation fractionation of free-radical polystyrene.

Polydisperse samples were prepared by the isothermal, uncatalyzed polymerization of styrene, both in bulk and in the presence of a transfer agent, ethyl benzene (*1, 9*). Samples prepared in this manner have distributions that are close to the most probable distribution.

In one case, a blend was made of two most probable distribution samples of widely different average molecular weight. The relative amounts of the two components were purposely chosen to yield a maximum value for $\overline{M}_z/\overline{M}_w$ in the blend and thereby exaggerate the high molecular weight tail of the distribution.

Molecular weight was determined by light scattering, osmotic pressure, and intrinsic viscosity measurements. The sources and properties of all samples are summarized in Table 1. Solutions were prepared with 99+% n-butyl benzene (*12*).

Viscosity measurements were made in the plate-cone geometry with a Weissenberg rheogoniometer. A platen diameter of 7.5 cm. and a cone angle of 0.5 deg. were used except when specified otherwise. Temperatures were maintained at 30°C. except in the several cases noted. Shear rates ranged from 0.01 to more than 1,000 sec.$^{-1}$. Apparatus calibration and the effects of different platen geometries were tested with Newtonian oils from the National Bureau of Standards. Shear rate, shear stress, and viscosity coefficient were calculated routinely for each combination of rotational speed and transmitted torque by using the standard equations for plate-cone geometry.

Viscosity measurements at high shear rates were invariably limited by the development of a flow instability at the rim of the platen. Extrusion of fluid from the gap began to occur with each solution somewhat beyond the shear rate region where viscosity first begins to decrease. In general, it was possible to penetrate deeper into the non-Newtonian region the smaller the cone angle, the higher the polymer concentration, and the higher the polymer molecular weight. Others have reported similar problems with plate-cone instruments (*13, 15*). All solution data used in this study were obtained prior to the onset of any visually observable instability at the rim.

Distribution and viscosity data for a polydisperse sample of polystyrene ($\overline{M}_z\overline{M}_{z+1}/\overline{M}_w^2 = 7.6$) were generously furnished by Arnold. The molecular weight distribution had been measured by gel permeation chromatography. Viscosity was measured on the undiluted polymer at 200°C.; data at low shear rates were obtained with a Weissenberg rheogoniometer and at high shear rates with an Instron capillary rheometer.

Distribution and viscosity data on three polydisperse samples

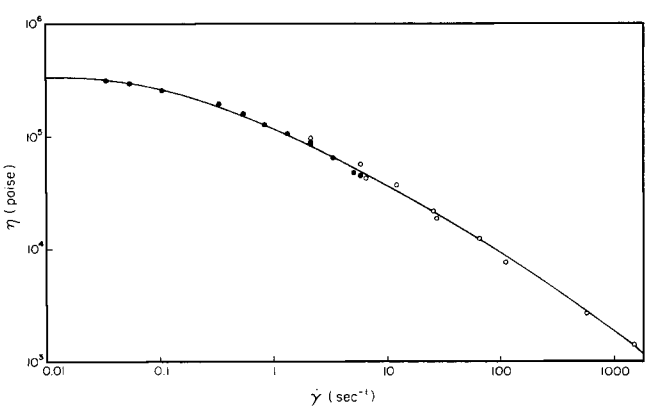

Fig. 4. Viscosity data on the broad distribution bulk polystyrene ($\overline{M}_w$ = 371,000). The closed circles are data obtained by rheogoniometer, the open circles by capillary rheometer. The solid line was calculated from the measured distribution by the entanglement theory and shifted parallel to the coordinate axes to best fit the data.

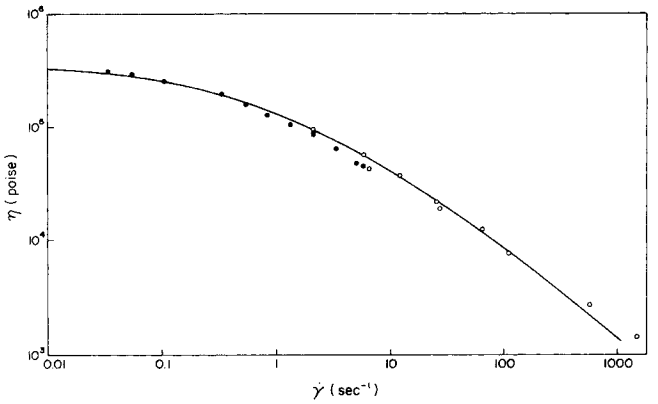

Fig. 5. Viscosity data on broad distribution bulk polystyrene. The data are the same as in Figure 4; the solid line was calculated from the measured distribution by Equation (9).

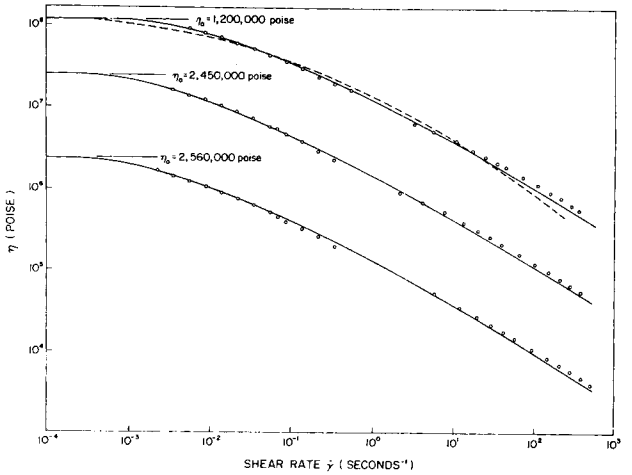

Fig. 6. Viscosity data on linear polyethylenes. The data have been displaced vertically to avoid crowding and overlap. The solid lines were calculated from the distribution by the entanglement theory. The dashed line on the top curve was calculated from Equation (9).

of linear polyethylene ($\overline{M}_z\overline{M}_{z+1}/\overline{M}_w^2$ = 49, 71, and 89) were furnished by Shida, Cancio, and Cote. Gel permeation again furnished the detailed distributions. Viscosities had been measured at 190°C. with a Weissenberg rheogoniometer and a CIL gas capillary rheometer. Corrections for diameter-length ratio and nonparabolic velocity profile were applied to all capillary data.

RESULTS AND DISCUSSION

All experimental curves of log η vs. log $\dot{\gamma}$ were shifted parallel to the axes to achieve the best possible superposition with master curves calculated from the entanglement theory. Figure 3 shows the dependence of viscosity on shear rate for different concentrations, molecular weights, and distribution breadths of the polystyrene solutions. The master curve for Z = 10 ($\overline{M}_w/\overline{M}_n$ = 1.09, $\overline{M}_z\overline{M}_{z+1}/\overline{M}_w^2$ = 1.26) was used for the samples with narrow distribution to allow for some polydispersity. The value Z = 0 (the most probable distribution) was used for the thermally polymerized samples. Good superposition was achieved in both cases, and indeed equally good superposition was obtainable with curves calculated from Middleman's equation.

The calculated master curve and experimental data on the blend are also shown in Figure 3. As pointed out earlier, this represents a case where the two theories give observably different shapes for the master curves. The agreement with the entanglement master curve is seen to be good. The Middleman curve, on the other hand, is too flat in the experimental region, and acceptable superposition was not attainable.

Figures 4 and 5 show the data on the undiluted polydisperse polystyrene. The range of η/η_0 values is considerably larger than in the solution data, so a larger portion of the master curve can be examined. The solid line in Figure 4 is the entanglement master curve, while that in Figure 5 was calculated from the Middleman equation. The tendency towards too small slopes at low shear rates and too large slopes at high shear rates is again evident in Figure 5, while good agreement over the entire range is found in Figure 4.

Figure 6 contains the data on the polyethylene samples. In these samples, the range of shear rates and η/η_0 values is very large. The positions of the curves were shifted vertically one or two orders of magnitude to avoid crowding the data. The true values of η_0 are given in Table 2. Agreement with calculated curves from the entanglement theory is still good, although there may be some slight tendency to underestimate the viscosity at the very highest shear rates. Actually, the shapes of the experimental curves are very similar, in spite of the differences in $\overline{M}_w/\overline{M}_n$ and $\overline{M}_z\overline{M}_{z+1}/\overline{M}_w^2$ among the samples. Likewise, the shapes of the calculated master curves $\left(\eta/\eta_0 \text{ vs. } \frac{\dot{\gamma}\tau_0}{2}\right)$ are similar, although slightly displaced from one another along the shear rate axis. The dashed line in Figure 6 is the best fit of the curve from Equation (9). Again, the deviations at the curve extremities are apparent.

Time constants were obtained by noting a value of $\dot{\gamma}\tau_0/2$ on the entanglement master curve and the corresponding value of $\dot{\gamma}$ on the experimental curve at superposition and by solving for τ_0. Values of τ_0 and the zero shear viscosity η_0 are given in Table 2. These results are supplemented by values obtained from recently reported measurements on undiluted polystyrenes with narrow distributions (23). The Z = 10 master curve was used to analyze these data. The fit was not as good as with the data reported here, especially in the high shear rate region where the viscosity was found to decrease more rapidly than the calculated curves. Nevertheless, the fit around the knee of the curve was good, and reasonably unambiguous values of τ_0 were obtained. Calculated values of the Rouse parameter for each system are also listed in Table 2.

It is clear that τ_0 and τ_R, although not numerically equal, are of the same order of magnitude, and that changes in one are paralleled closely by changes in the other. Further examination of the polystyrene data reveals that, regardless of the molecular weight distribution, the ratio of τ_0/τ_R varies systematically with both concentration and molecular weight. Measurements on narrow distribution polystyrenes alone led to Equation (4), according to which τ_0/τ_R vs. the product cM yields a single straight line for systems of various concentrations and molecular weights. In both viscosity theories, the appropriate expression for the Rouse relaxation time in polydisperse systems is

$$\tau_R = \frac{6}{\pi^2}\,\frac{\eta_0\,\overline{M}_w}{cRT} \qquad (16)$$

However, it is by no means obvious what average molecular weight should be used in the product cM for polydisperse systems, since the cM term in Equation (4) is essentially empirical.

It was found that a unique curve could be obtained with $c\overline{M}_w$ as the correlating variable. Figure 7 shows τ_R/τ_0 as

Table 2. Summary of Flow Parameters for Polystyrene Systems (Measurements at 30°C. Unless Otherwise Noted)

$\overline{M}_w$	c, g./ml.	η_0, poise	τ_0, msec.	τ_R, msec.
	Narrow distribution samples			
48,500	undiluted (b)	19,000	16.0	15.2
97,000	0.55	364	2.15	1.55
117,000	undiluted (c)	25,700	47.3	42.0
160,000	0.55	2,870	20.0	20.1
179,000	undiluted (c)	109,000	230.0	304.0
217,000	undiluted (c)	190,000	374	658
242,000	undiluted (c)	295,000	700	1,110
411,000	0.255	92.5	3.5	3.59
	0.30	284.0	8.6	9.37
	0.35	763	19.0	21.5
	0.40	1,940	39.0	48.0
	0.45	6,080	102.0	134.0
	0.50	17,500	226.0	346.0
	0.55	48,500	550	872.0
860,000	0.20	255.0	21.0	26.4
	0.255	1,150	64.0	93.3
	0.30	3,600	150.0	248.0
	0.35	9,600	290.0	568
	0.45	71,000	1,240	3,260
	0.55	470,000	6,400	17,700
2,400,000	0.255	40,900	2,700	9,260
	Broad distribution samples			
160,000	undiluted (d)	1,200,000	2,560	4,000
192,000	undiluted (d)	2,560,000	7,270	10,200
198,000	undiluted (d)	2,450,000	8,000	10,100
209,000	0.40	155.0	3.7	1.95
241,000	0.20	4.5	0.10	0.13
371,000	undiluted (e)	330,000	1,080	1,910
418,000	0.30	72.0	0.52	2.42
677,000	0.255	88.0	4.0	5.64
	0.40	2,000	56.0	81.5
1,900,000	0.255	11,700	790	2,100
	0.255 (a)	7,500	580	1,270
	0.35 (a)	76,000	2,800	9,320
3,370,000	0.20	520	53.0	212.0

(a) Measured at 50°C.
(b) Measured at 159°C.
(c) Measured at 183°C.
(d) Measured at 190°C. (polyethylene samples).
(e) Measured at 200°C.

a function of $c\overline{M}_w$. With the exception of the value for the blend, the results on all polystyrene samples are well represented by a single straight line. This provides an important and essential test of the calculated master curves and the underlying theory, namely, that the relaxation times which are obtained by superposition correlate with the properties of the solutions in a manner which is independent of molecular weight distribution.

The fit between the data for the blend and the entanglement master curve is quite good, as noted earlier, but the derived relaxation time is much smaller than expected from the behavior of the other systems. The reasons for the distinction are not clear, and further experiments with broad distribution mixtures are needed.

Time constants were also obtained with master curves from Equation (9). All values of τ_0 were larger than obtained with the entanglement curves, the narrow distribution ($Z = 10$) by a factor of 1.06, and the most probable distribution ($Z = 0$) by a factor of 1.75. Values for the blend and the undiluted polydisperse sample were more difficult to establish because of lack of fit with the calculated curves. The best factors by a visual fit were 4.6 and 3.1, respectively.

The correlating variable $c\overline{M}_n$ came closer than $c\overline{M}_w$ to yielding a single curve for all data. Figure 8 shows τ_R/τ_0 vs. $c\overline{M}_n$, the τ_0's in this case having been obtained by applying the factors above to the τ_0 values in Table 2. It is noteworthy that in this correlation the time constant for the blend agrees much better with values from the other systems than in Figure 7. On the other hand, the undiluted polydisperse sample is now displaced somewhat, and the general degree of scatter at low $c\overline{M}_n$ values seems greater than Figure 7. It seems best to suspend judgement on this point until more data on polydisperse systems can be examined.

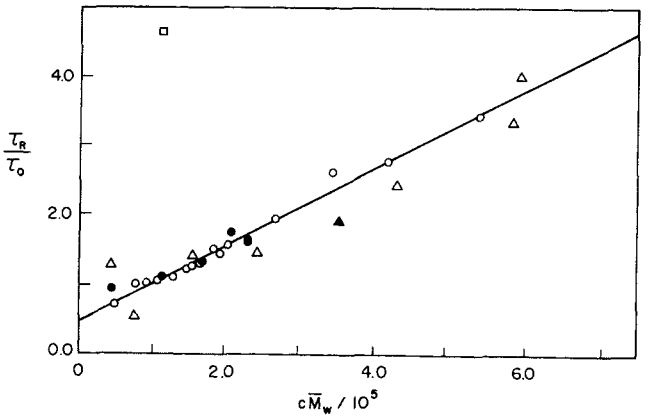

Fig. 7. Time constant ratio from entanglement theory vs. $c\overline{M}_w$. Solutions are represented by open symbols, bulk polystyrenes by closed symbols. Specifically: blend (□), broad distribution bulk sample (▲), narrow distribution solutions (○), narrow distribution bulk samples (●), most probable distribution solutions (△).

At least two interpretations of the cM product are possible. Williams' recent theory of nonentangled polymer solutions (25) suggests that the ratio of dilute solution relaxation time, in this case τ_R, to concentrated solution relaxation time τ_0 should be directly proportional to the product cM. Although the Williams result has not been generalized to include polydisperse systems, the nature of the molecular mechanism suggests that an average molecular weight such as $\overline{M}_n$ or $\overline{M}_w$ might well be appropriate.

The product cM can also be viewed as representing the entanglement density of the system. According to current theories of zero shear viscosity, the density of chain entanglements is proportional to cM and in polydisperse systems to the product $c\overline{M}_w$ (7, 20). The average number of entanglement points per molecule is

$$E = 2\,\frac{c\,\overline{M}_w}{(cM_c)} \qquad (17)$$

and for polystyrene systems the product cM_c is approximately 35,000 (20). This latter interpretation, or at least its terminology, will be retained for the present because all systems in this study are in the entanglement region, judged by the entanglement densities calculated from Equation (17).

The line in Figure 7 was calculated by least squares from the data on the narrow distribution samples. The product $c\overline{M}_w$ was replaced by entanglement density E [Equation (17)], yielding the result

$$\tau_R/\tau_0 = 0.50\,(1 + 0.17E) \qquad (18)$$

This equation suggests a number of conclusions. It implies that solutions with equal entanglement densities will have experimental relaxation times which are directly proportional to their theoretical Rouse parameters, regardless of the molecular weight distribution of the polymers. Also, at sufficiently high entanglement densities the experimental relaxation time should become independent of average

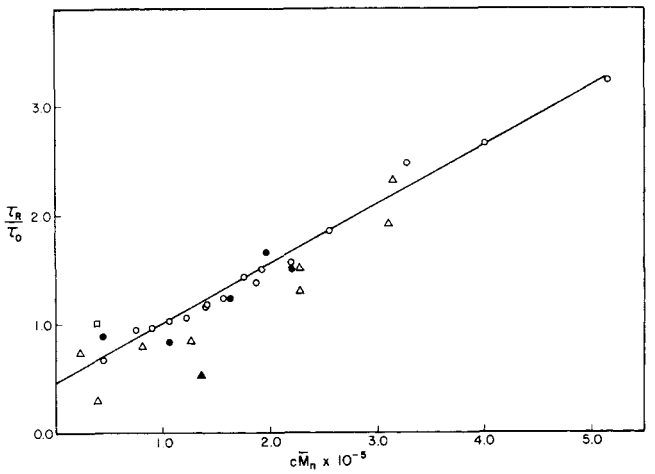

Fig. 8. Time constant ratio from Equation (9) vs. $c\bar{M}_n$. Symbols are the same as Figure 7.

molecular weight and proportional to the inverse square of concentration, again regardless of the distribution of molecular weights. This conclusion is consistent not only with the molecular time constant recently suggested by Williams (*25*), but also with observations on other polymer systems (*4, 16*).

The good agreement between calculated and experimental results for samples of different distribution breadths supports the averaging process that was developed through the entanglement theory. Furthermore, systematic deviations appear at higher distribution breadths in curves obtained in another way [Equation (9)], which suggests that the averaging technique is indeed important in obtaining good agreement with experiment.

ACKNOWLEDGMENT

This work was supported by grants from the Petroleum Research Fund, the National Science Foundation, and the Advanced Projects Agency of the Department of Defense through the Northwestern University Materials Research Center. Fellowship support by the National Aeronautics and Space Administration is also gratefully acknowledged. We are indebted to Dr. Kenneth Arnold of Shell Development Company and to Dr. Mitsu Shida, Dr. James Cote, and Leo Cancio of Chemplex Company for furnishing data used in the paper and for helpful discussions regarding the results. Conversations with Dr. Guy Berry of Carnegie-Mellon University and William Uy of Northwestern University were also helpful.

NOTATION

c = polymer concentration, g./ml.
E = entanglement density, entanglement points per molecule
$F(\dot{\gamma})$ = function defined in Equation (14)
g = function defined in Equation (6)
h = function defined in Equation (7)
K = multiplying factor of order unity
M = polymer molecular weight
M_c = critical molecular weight in melt viscosity
$\bar{M}_n$ = number average molecular weight, $\int_0^\infty P(n)\,dn / \int_0^\infty P(n)\,dn$
$\bar{M}_w$ = weight average molecular weight, $\int_0^\infty n^2 P(n)\,dn / \int_0^\infty n P(n)\,dn$
$\bar{M}_z$ = z average molecular weight, $\int_0^\infty n^3 P(n)\,dn / \int_0^\infty n^2 P(n)\,dn$
$\bar{M}_{z+1}$ = $z+1$ average molecular weight, $\int_0^\infty n^4 P(n)\,dn / \int_0^\infty n^3 P(n)\,dn$
n = number of repeating units in polymer chain, degree of polymerization
n_n = number average degree of polymerization
n_w = weight average degree of polymerization
$P(n)$ = distribution function, fraction of polymer chains with n repeating units
R = universal gas constant
T = absolute temperature
Z = parameter in Zimm-Schulz distribution, Equation (15)

Greek Letters

$\dot{\gamma}$ = shear rate, sec.$^{-1}$
$\dot{\gamma}_0$ = characteristic shear rate, experimental parameter, sec.$^{-1}$
η = viscosity, poise
η_0 = viscosity at zero shear rate, poise
$\varphi\left(\frac{\dot{\gamma}\tau_0}{2}\right)$ = viscosity master curve for monodisperse polymer
θ = intermediate variable in viscosity calculation
τ_B = Bueche time constant, $12\,\eta_0 M/\pi^2 cRT$
τ_0 = experimental time constant
τ_R = Rouse time constant, $6\eta_0 M/\pi^2 cRT$

LITERATURE CITED

1. Alberino, L. M., Ph.D. thesis, Northwestern Univ., Evanston, Ill. (1966).
2. Bueche, F., "Physical Properties of Polymers," Interscience, New York (1962).
3. ———, and S. W. Harding, *J. Polymer Sci.*, **32**, 177 (1958).
4. Dewitt, T. W., H. Markovitz, F. J. Padden, Jr., and L. J. Zapas, *J. Colloid Sci.*, **10**, 174 (1955).
5. Ferry, J. D., "Viscoelastic Properties of Polymers," Wiley, New York (1961).
6. Flory, P. J., "Principle of Polymer Chemistry," Cornell University Press, Ithaca, N. Y. (1953).
7. Fox, T. G., and V. R. Allen, *J. Chem. Phys.*, **41**, 344 (1964).
8. Fox, T. G., and G. C. Berry, *Advan. Polymer Sci.*, **5**, 261 (1968).
9. Gandhi, A., M. S. thesis, Northwestern Univ., Evanston, Ill. (1966).
10. Graessley, W. W., *J. Chem. Phys.*, **43**, 1942 (1965).
11. *Ibid.*, **47**, 1942 (1967).
12. Graessley, W. W., R. L. Hazelton, and L. R. Lindeman, *Trans. Soc. Rheology*, **11**, 267 (1967).
13. Hutton, S. F., *Nature*, **200**, 646 (1963).
14. Kataoka, T., *J. Polymer Sci.*, Part B, **5**, 1063 (1967).
15. King, R. G., *Rheol. Acta*, **5**, 35 (1966).
16. Kraus, G., and Gruver, *J. Polymer Sci.*, Part A, **2**, 797 (1964).
17. Leaderman, H., R. G. Smith, and L. C. Williams, *ibid.*, **36**, 233 (1959).
18. Lodge, A. S., "Elastic Liquids," Academic Press, London, England (1964).
19. Middleman, S., *J. Appl. Polymer Sci.*, **11**, 417 (1967).
20. Porter, R. S., and J. F. Johnson, *Chem. Rev.*, **66**, 1 (1966).
21. Porter, R. S., M. J. R. Cantow, and J. F. Johnson, *Trans. Soc. Rheology*, **10**, 621 (1966).
22. Ree, T., and H. Eyring, *J. Appl. Phys.*, **26**, 793, 800 (1955).
23. Stratton, R. A., *J. Colloid Interface Sci.*, **22**, 517 (1966).
24. Toelcke, G. A., K. F. Madonia, C. G. Gogos, and J. A. Bienenberger, *Polymer Eng. Sci.*, **7**, 318 (1967).
25. Williams, M. C., *AIChE J.*, **12**, 1064 (1966).
26. *Ibid.*, **13**, 534 (1967).

Manuscript received May 8, 1968; revision received September 4, 1968; paper accepted September 20, 1968. Paper presented at AIChE New York City meeting.